GIS-based modelling of electric-vehicle–grid integration in a 100 % renewable electricity grid

Mengyu Li[a,*], Manfred Lenzen[a], Dai Wang[b] , Keisuke Nansai[a,c]

[a] ISA, School of Physics A28, The University of Sydney, NSW 2006, Australia

[b] Tesla Inc. 3500 Deer Creek Rd, Palo Alto, California, USA

[c] Center for Material Cycles and Waste Management Research, National Institute for Environmental Studies, 16-2 Onogawa Tsukuba, Ibaraki 305-8506, Japan

Abstract: We examine the spatio-temporal interactions of widespread electric vehicle (EV) charging with a future, 100% renewable electricity system in Australia. More specifically, we use a GIS-based electricity supply-demand model simulating an hourly competitive-bidding process over an entire year. We obtain least-cost grid configurations that include both renewable energy (RE) generators and EVs, the latter under both uncontrolled and controlled charging, and adoption rates between 0 and 100%. We characterise the vehicle-to-grid interaction in terms of overall installed capacity, hourly generation and spillage, levelized cost of electricity (LCOE), as well as transmission network expansion topology. We show that supplying 100% renewable electricity to cover current electricity needs in Australia, as well as powering all Australian passenger vehicles as controlled-charged EVs, requires 205 GW of installed capacity at an LCOE of 14.7 AUD¢/kWh. This 100% RE supply with EV charging leads to a reduction in electricity cost of 1,086 AUD/capita annually, comparing to the current annual expenditure for electricity and conventional vehicle fuel.

Keywords: Low-carbon electricity supply, Electric vehicles, Vehicle-to-grid integration, GIS

[*] Corresponding author. Email address: meli0258@uni.sydney.edu.au

1. Introduction

In the IPCC's special report on climate change, increasing the generation of electricity from renewable energy (RE) resources along with rapidly declining the carbon-intensive end-user sectors are essential to its 1.5°C mitigation pathways [1]. The transportation sector, accounting for 28% of global final energy supply, 23% of world energy-related CO_2 emissions [2] and 65% of global oil consumption [3], features prominently in deep-decarbonization mitigation pathways. Replacing gasoline and diesel cars by electric vehicles (EVs) provides a potential solution for CO_2 emission reduction and transportation decarbonization [4].

However, due to the variability of wind and solar resources, the massive adoption of RE sources in electricity generation poses challenges in balancing generation, demand, storage, and transmission. Low wind and solar resource periods require installed capacity of renewable grids to be 3-5 times the demand, leading to significant capital cost [5]. Because their demand occurs during peak hours, EVs have the potential to exacerbate these challenges further, especially when their charging is unconstrained [6]. It is therefore necessary to investigate which configurations of energy carriers and generator sites would allow integrating large numbers of EVs under different charging strategies, and how reliable and cost-effective these configurations would be.

Most of the existing studies examining the impact of EV charging on power grids mainly focus on small virtual distribution networks or microgrids/energy hubs by considering a limited number of EVs (e.g., hundreds [7-12] or thousands [13-17]) operating for short simulation periods (e.g., 24h in [7-10, 12-16] and five days in [17]), providing limited information on how the actual grid operations would be affected by the more widespread adoption of EVs.

A limited number of studies examine the vehicle-grid-integration (VGI) impact based on real-world regional grid operation settings. Examples include the VGI impacts on the New York Independent System Operator's (NYISO) energy market with modelling periods of 20 [18] or 21 days [19] and no spatial resolution, on the Victorian residential electrical network covering 250 dwellings [20], on a UK urban underground network spatially distinguished by different location types (i.e., residential, commercial, industrial) [21] operated during a typical day, and two Italian provincial grids [22] temporally averaged to one day. The spatial scale of these regional studies provide limited information on the planning of the utility's transmission & distribution (T&D) for the entire service territory that are often regional-interconnected [23].

In addition, most of these regional studies only focus on the VGI impacts on the demand profiles [20-22], with limited details on the efficient operation and economical capital and T&D expansion of the power delivery system.

Recently, a few studies attempt to model the VGI impact on a national grid system, with examples covering Northern Europe [24], Germany [25], Scandinavia and Germany [26] and the Netherlands [27]. Due to a large number of time and space variables involved in modelling grid operation and EV charging, most of these studies made some simplifications regarding spatial or temporal resolution. The temporal resolution is limited to time slices of 2 days [27], 20 days [26] and seven weeks [24]. The spatial distribution of generators and transmission is either not considered [25, 27] or just expressed at a low spatial resolution by five sub-regions [24] and 14 regions [26]. In order to provide more validated and reliable sittings of future T&D equipment and the power stations, the whole-of-grid operation model with sufficient spatial precision and temporal resolution is important [28]. Besides, all of these studies consider a specific scale of fossil energy as a backup when modelling the national grid operation (e.g., 30% - 83% from coal and gas [24-27]), thus leaving open the question of how a 100% renewable grid would perform under different EV penetration rates.

As one of the most coal-dependent countries worldwide, Australia presents a compelling case for examining the decarbonisation potential for its electricity grid and transport sector. In Australia, the Renewable Energy Target (RET) requires that 23.5% of Australia's electricity changes into renewable energy sources by 2020 [29]. Other regional governments set more ambitious targets, such as 50% electricity produced from RE resources in South Australia (SA) by 2025 [30], and 100% electricity consumed in the Australian Capital Territory (ACT) by 2020 [31]. In terms of transport sector electrification, SA is targeting 30% - 40% of its fleet to be EVs by 2019 to 2021 [32]. EV sales are forecast to reach 615 thousand vehicles per annum by 2030, increasing to 1.89 million annual new vehicle sales by 2040 [32]. It is, therefore, timely and meaningful to model the EV interaction with a national 100% renewable power system in Australia.

Against the above background, this study aims to evaluate spatio-temporal VGI impacts on a 100 % renewable electricity supply system in Australia under various EV adoption rates. To this end, we utilise a GIS-based integrated electricity supply-demand model to simulate the hourly competitive-bidding process based on renewable resource availability and generator

cost. The model covers the whole continent of Australia over an entire year, and is able to quantify in detail the VGI characteristics in terms of the overall installed capacity, hourly generation and spillage, energy carrier mix, transmission network expansion topology, as well as levelized cost of electricity (LCOE) of the national RE-based power grid. Specifically, the contributions of this paper are threefold:

1. We demonstrate the computational capability to search for high-resolution spatial and temporal configurations of the national least-cost power supply coupled with large-scale EV charging.
2. In contrast to previous studies [24-27] considering fossil energy as a backup, we investigate EV charging at a disaggregated level on a 100% RE grid in Australia.
3. We are able to quantify in detail the VGI impacts on capital and T&D expansion cost of the power delivery system, together with GIS representations of new transmission networks and power stations for the future RE-based national power grid.

This study is directly relevant to efforts in the large-scale deployment of renewable energy (RE) and EVs in Australia. A critical issue in future 100% renewable grids is the installed capacity of generators, because this quantity impacts directly on investment cost. Here we show how the charging mode of EVs has a bearing on total installed capacity, and this is certainly a feature of our results that needs to be taken into account, for example by system operators, energy ministries, and transport officials alike. Moreover, it demands that transport and power planners work together to achieve an optimal integration of a 100% renewable grid and widespread penetration of EVs. More specifically, our model outputs allow the identification of areas with high installed capacity or transmission line capacity in preparation for future investment plans, and this will be useful for attracting investment into power infrastructure into the most critical areas. Our findings can also contribute to public advocacy in confirming viewpoints about the feasibility of a 100% - RE system powering all Australian passenger vehicles as EVs.

2. Methodology

2.1 Overview of the model

The overall integrating framework consists of three sub-models to determine the lowest Levelized Cost of Electricity (LCOE) configuration of the Australian grid under different EV charging schemes with various EV adoption rates (Fig. 1). First, the Energy Resources Model computes the hourly generation potential by location and RE resources, together with its

bidding price, based on the input installed capacity, weather and cost data [33-37]. Second, the demand model estimates the hourly electricity demand including EVs' charging demand in addition to non-EV demand, based on South East Queensland Travel Survey (SEQTS) [38] and Australian Energy Market Operators (AEMO) historical hourly electricity demand data [39], respectively. Third, the supply-demand dispatch model then simulates the hourly competitive-bidding process based on those intermediate outputs, i.e., the generation potential, costs, and demand. The gridded-locations are defined by 390×479 raster data (8.9 × 8.9 km per grid box), covering the whole of Australia in GIS.

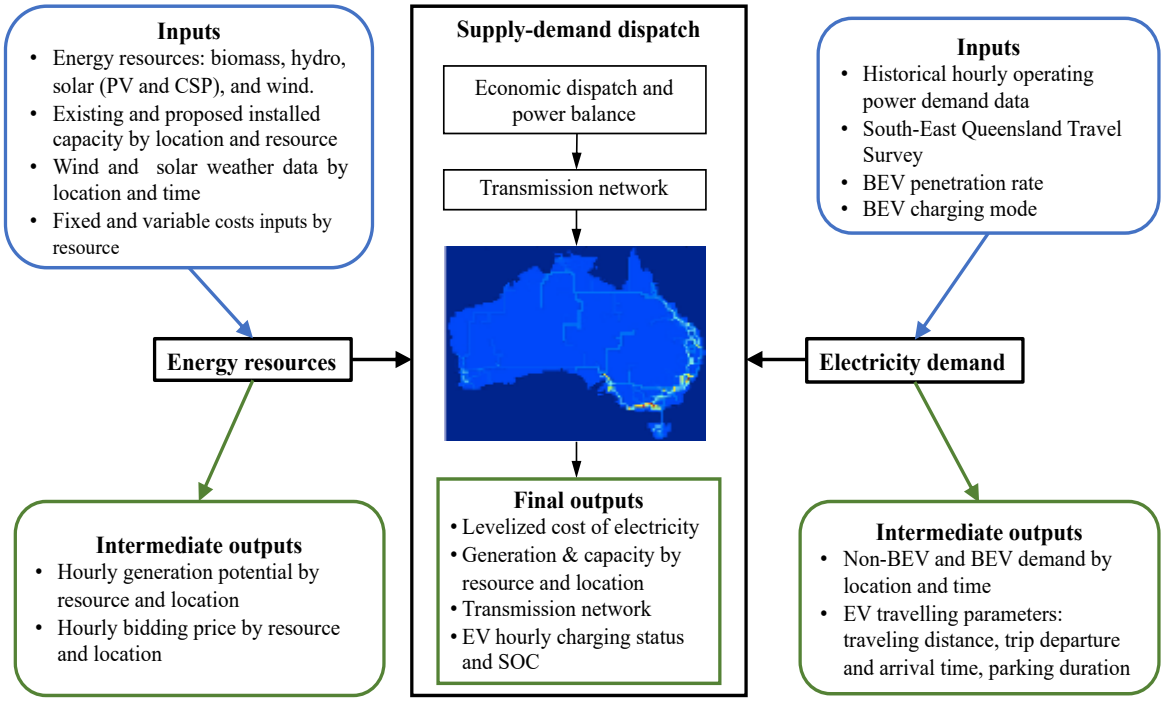

Fig. 1 Overview of the integrated power grid model. *Blue box: model input data; green box: intermediate and final outputs; black box: three sub-models.*

The overall optimisation goal is to minimise the LCOE (AUD$) formulated by Equation (1). The LCOE is the sum of the total capital and fixed costs of installed infrastructure and the variable and fuel costs of electricity generation and transmission/distribution.

$$LCOE = \left\{ \sum_{f=1}^{Fuel} \sum_{g=1}^{Grid} (c_{capt} + c_{fix}) \cdot Cap(f,g) + \sum_{f=1}^{Fuel} \sum_{r=1}^{Grid} \sum_{t=1}^{T} (c_{var} + c_{fuel}) \cdot Gen(f,g,t) + \sum_{tr=1}^{Line} c_{line} \cdot Cap(tr) \right\} \div \sum_{f=1}^{Fuel} \sum_{r=1}^{Grid} \sum_{t=1}^{T} Gen(f,g,t) \quad (1)$$

where, c_{capt} and c_{fix} are the capacity and fix cost per kW (AUD$/kW) for fuel type *f* installed

at grid g, c_{var} and c_{fuel} are the variable operating and maintenance and fuel cost per kWh (AUD$/kWh) electricity generated. c_{line} is the transmission cost per kW (AUD$/kW), $Cap(f,g)$ and $Cap(tr)$ are the capacity (in kW) carried at location g and grid transmission line tr, and $Gen(f,g,t)$ is the hourly electricity dispatched (in kWh) for fuel type f at location g at hour t within an entire year (t=1,2,…8760). The considered power generation from 6 renewable energy carriers are biomass, hydro, solar PV (utility-scale and rooftop), concentrating solar power (CSP, with 15 hours heat storage capacity), and wind (i.e., f=1, 2, …, 6).

The primary optimisation constraint is the balancing between the total hourly demand and the generation subtracting generation overheads $ov_{g,l}$ between generator at location g and demander at l by Equation (2). Here, $DM_{non\ EV}(l,t)$ and $DM_{EV}(l,t)$ denote the non-EV and EV demand at location l, respectively.

$$\sum_{f=1}^{Fuel}\sum_{g=1}^{Grid} Gen(f,g,t) = \sum_{l=1}^{Demand\ location} \left(DM_{non\ EV}(l,t) + DM_{EV}(l,t)\right) ov_{g,l}, \forall t \subseteq [1,\cdots,8760] \quad (2)$$

Equation 3 determines the generation overheads due to transmission and distribution losses ($TL_{g.l}$) and reserve margin (RM) requirements of 15% [33, 34]. Transmission losses are estimated based on the transmission line distance between locations g and l ($tr_{g,l}$), assuming unit transmission loss of 1% loss per 100 miles [33]. Distribution losses are estimated at 5.3% of the end-use demand at each grid cell [33].

$$ov_{g,l} = \frac{1+RM}{1-TL_{g.l}} \quad (3)$$

For each sub-region g, the maximum of the generation ($Potential(f,g,t)$) is limited by natural factors (e.g., rainfall, wind, and irradiance) as the following equation.

$$Potential(f,g,t) > Gen(f,g,t), \forall f \subseteq [1, Fuel] \text{ and } \forall g \subseteq [1, Grid] \quad (4)$$

2.2 Energy resources modelling

We apply the energy resources model developed by Lenzen et al. [40-42] to estimate the hourly potential generation ($Potential(f,g,t)$) and the bid covering fixed and variable costs for electricity generation, storage and transmission for each energy resource f at each gridded-location g (see yellow border-box in Fig. 2). To thoroughly examine the interaction of the EVs with the intermittent RE sources, we assume that PV, CSP, and wind can grow to their resource potential, but hydro and biomass of dispatched energy carriers were restricted to their existing

capacity. We then estimate the potential generation for non-dispatched energy carriers (wind, PV and CSP) based on the real-time weather condition at each location. While, for fully-dispatchable ones, the estimate uses their installed capacity.

We fix the bid for each generator before performing the generator competitive-bidding process in the supply-demand dispatch model. Variable and fuel costs are based on per kWh generation, while capital, fixed and transmission cost are on kW basis as shown in Equation 1. They are all decision variables that can be determined with the knowledge of the actual power flow of the grid system running over the entire period. Alternatively, we estimated the bid for each generator based on the cost input assumptions listed in Table 1 for various power generation technologies in the first loop. At the end of each simulation, in the supply-demand dispatch model, we re-calculate the cost for each generator based on the real-time operation and transmission/distribution loss within the entire year and then exclude uneconomic generators (see Fig. 2 for the step-by-step process of the model).

Table 1: Cost input assumptions for various power generation technologies [33, 34]

Fuel type	**Capital cost ($ kW^{-1})**	**Fixed O&M cost ($kW^{-1}yr^{-1})**	**Variable cost ($ kWh^{-1})**	**Fuel cost ($ MWh^{-1})**	**Capacity factor**	**Life-time (yr)**	**Total cost ($ MWh^{-1})[a]**
Biomass	5350	109	7	1.5	0.85	45	38.8
Hydro	5114	48	6.7	0	0.85	55	26.2
Wind	2693	35	10.5	0	0.4	25	52.5
PV	1342	33	0	0	0.22	30	45.5
CSP 15 h storage	6256	68	13.1	0	0.6	30	67.2
Rooftop PV[1]	1075	22	0	0	-	-	-

a: Total cost is the basis for bids is given as [capital cost × (1+δτ)/(8760 h/yr × Lifetime) + fixed O&M cost/8760 h/yr] / capacity factor + variable cost + fuel cost, where τ=8% is the assumed interest rate, and δ=50% is the debt fraction.

[1] Rooftop PV does not participate in the bidding process.

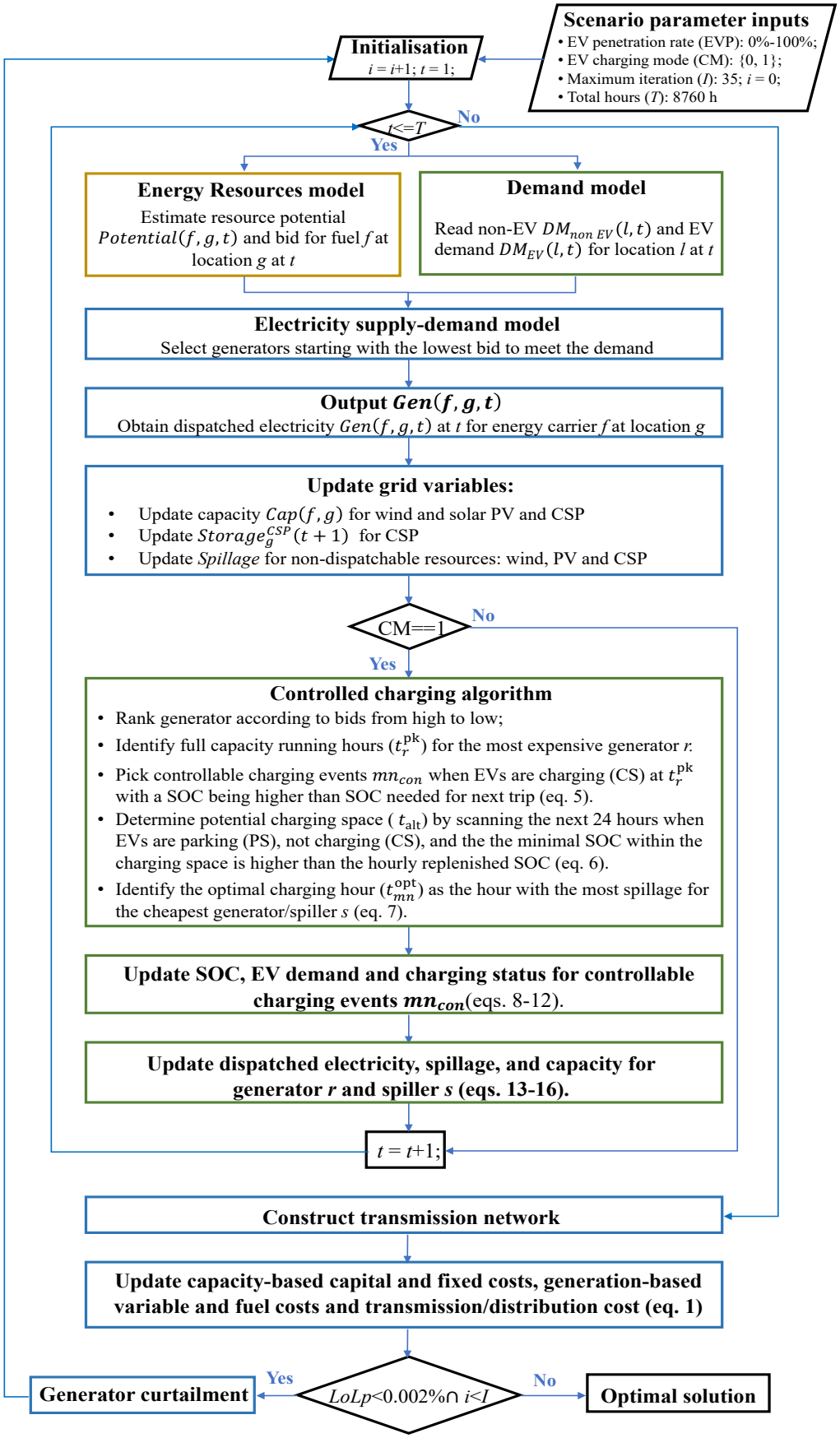

Fig. 2 Flowchart of the integrated power grid model. *Yellow box: energy resources model; green box: demand model; blue box: electricity supply-demand model.*

2.3 Demand modelling

We calculate the EV charging load using a GIS-based EV charging model developed by Li et al. [43, 44]. The model combines real-world South-East Queensland Travel Survey [38] with GIS-based topography data at a country scale. Non-EV electricity demand refers to Australian Energy Market Operators (AEMO) historical data on hourly electricity demand [39] (see green box in Fig. 2).

Specifically, the SEQTS contains detailed travel behaviour information including vehicle ID, trip ID, trip departure time, distance, arrival time and parking time, and SA1[2] codes (short for Statistical Area Level 1) of departure and arrival places associated with 26,196 vehicles with 108,913 trips collected from April 2009 up to May 2012 [38]. We use the three-year travel data to create a weekly driving and charging profile for each vehicle grouped by weekdays and weekends, with the charging located at different SA1 regions. We then map the charging load for South East Queensland (SEQ) area to the 390×479 raster grids by overlaying the digital boundary of each SA1 code onto the GIS-gridded data.

No national travel survey was available in Australia [45]. Hence, in a manner similar to our previous work [43], we develop a probabilistic model to expand the EV charging demand from SEQ to whole Australia by capturing the coupled relationship of the joint probability between these temporal-spatial variables. This probabilistic model allows defining yearly driving and charging profiles for EVs at locations outside SEQ, with each EV being provided with a unique yearly travelling pattern. The pattern characterizes hourly parking status $PS(t)$ (binary matrix, 0 = not charging, 1 = charging) and travel distance $TD(t)$ along with the hourly charging status $CS(t)$ (binary matrix, 0 = not charging, 1 = charging), state-of-charge (SOC) status $SOC(t)$ at every $0<t<8760$h.

We estimate the EV charging demand under both uncontrolled and controlled charging. The former assumes that EVs charge immediately after parking and continue charging until the battery is full or the next trip starts. The latter is defined by a charging pattern that limits the "controllable extent" of the EV charging events. This controllable extent of the charging space is constrained both by the driving patterns and SOC status of each EV. An EV n with a predicted parking time ($t_{\mathrm{p},mn}$) shorter than the recharging periods for satisfying the SOC required for the next trip (with a travel distance $t_{\mathrm{d},(m+1)n}$) must be charged throughout the parking period. Those

[2] SA1 (short for Statistical Area level 1) code is designed as the smallest unit for the release of Census data in Australia.

charging events mn_{uncon} (m: trip index; n: EV index) have no flexibility for re-scheduling and are defined as "uncontrollable charging events" by Equation 5.

$$mn_{\text{uncon}}=\{SOC\left(t_{a,mn}\right)+SOC\left(t_{p,mn}\right)<SOC_{m+1,n}\} \tag{5}$$

In contrast, controllable charging events can be rescheduled to minimise system LCOE, and are defined by those EVs with a parking time longer than the charging hours needed for the next trip. The potential charging space (t_{alt}) is constrained by scanning the next 24 hours when EVs are parking, not charging, and the minimal SOC within the charging space is higher than the hourly replenished SOC as Equation 6.

$$t_{\text{alt}}=\left\{\begin{matrix} CS_{mn}\big((t+1):(t+24)\big)=0\cap PS_{mn}\big((t+1):(t+24)\big)=1 \\ \cap SOC_{mn}(t)>SOC_{m+1,n}\cap SOC_{mn}\big((t+1):(t+24)\big)>SOC(1) \end{matrix}\right\} \tag{6}$$

Scanning 24-hour window guarantees EVs to have the same SOC level with uncontrolled charging after one full day's controlled charging, resulting in an unchanged total amount of EV charging load under different charging scenarios. Limiting the minimal SOC by the hourly replenished SOC ensures SOC >0 for any $t\subseteq[1,8760]$ under controlled charging.

2.3 Integrated low carbon grid modelling

An integrated supply-demand dispatch model represents the grid operation (blue box in Fig. 2). It simulates an hourly competitive-bidding process by dispatching the electricity generated from the energy resources model to meet hourly demand including EV load from the demand model. After the economic dispatch at t, we update the actual electricity generation, capacity, storage for CSP, and spillage according to the real-time electricity dispatch outputs. At the end of the simulation period, we construct the expanded transmission network ~~utilising accelerated link-distance functions~~ based on the actual power flow. Transmission cost for each generator can then be allocated based on the network capacity participation.

We then exclude generators based on their cost efficiency over the modelling period. The model iterates with uneconomic generators being excluded until a stable configuration is achieved without any generators being excluded over the spatial and energy carrier search space within the latest three loops, and the variation in hourly generation cost fell below $0.001 per

MWh.

Under uncontrolled charging, EV charging profiles are assumed to be independent of the grid scheduling and are added deterministically to the based demand without EVs. In contrast, EVs can reschedule their charging within the "charging space" under controlled charging. To be specific, after a run under uncontrolled EV charging, the supply-demand dispatch model identifies and passes full capacity running hours (t_r^{pk}) for generator *r* (starting with the lowest cost-efficiency one) to the demand model. The demand model will then identify EVs charging at t_r^{pk} and re-schedule these charging events based on their "controllable extent" (t_{alt}, Equations 5-6) only if this reduces overall electricity system cost. The optimal charging hour within the charging space t_{alt} is then determined as the hour when a cheap generator (starting from the highest cost efficiency spiller *s*) spills the most as Equation 7.

$$t_{mn}^{\mathrm{opt}} = \max\left(Spillage_g^s(t_{alt})\right) \tag{7}$$

As a result, our controlled charging strategy shifts the generation of a higher-cost generator *r* at time t_r^{pk} with the spillage of a lower-cost generator *s* within a set of alternative charging hours t_{alt}, and reduces the capacity and generation of expensive generators by making use of the spillage from cheap spillers. In essence, our controlled changing utilises the "controllable extent" (t_{alt}) as a rolling horizon, in order to differentiate the controlled charging demand curve for each vehicle and to reduce the computational complexity.

After controlled charging scheduling, system variables both for EVs including its SOC within peak and shifted hour (Equation 8), the corresponding charging demand (Equations 9-10) and charging status at peak and shifted hour (Equations 11-12). Then the model updates the power system variables including the hourly dispatch electricity generation (Equations 13-14) and spillage for generator and spiller (Equations 17-18) and capacity for generator *r* (Equations 15-16), respectively. The bid of generators affect EV charging scheduling and thus the charging demand. The shifted controlled EV charging demand, in turn, affects the spatio-temporally distributed lowest-cost configuration of the generators.

$$SOC_{mn}\left(t_r^{pk}:\left(t_{mn}^{opt}-1\right)\right) = SOC_{mn}\left(t_r^{pk}:\left(t_{mn}^{opt}-1\right)\right) - SOC(1) \tag{8}$$

$$demand_g^{EVP}(t_r^{pk}) = demand_g^{EVP}(t_r^{pk}) - charging\ rate \tag{9}$$

$$demand_g^{EVP}(t_{mn}^{opt}) = demand_g^{EVP}(t_{mn}^{opt}) + charging\ rate \tag{10}$$

$$CS_{mn}(t_r^{\mathrm{pk}}) = 0 \tag{11}$$

$$CS_{mn}(t_{mn}^{\mathrm{opt}}) = 1 \tag{12}$$

$$Generated_g^r(t_r^{pk}) = Generated_g^r(t_r^{pk}) - charging\ rate/transmission\ loss_g^r \tag{13}$$

$$Generated_g^s(t_{mn}^{\mathrm{opt}}) = Generated_g^s(t_{mn}^{\mathrm{opt}}) + charging\ rate/transmission\ loss_g^s \tag{14}$$

$$Capacity_g^r = \max(Capacity_g^r,\ Generated_g^r(t)/resourcefactor_g^r(t)) \tag{15}$$

$$Spillage_g^{r,s}(t) = Capacity_g^{r,s} \cdot resourcefactor_g^{r,s}(t) - Generated_g^{r,s}(t) \tag{16}$$

2.4 Scenario setting

We employ the driving and battery performance parameters from Tesla, because this brand has emerged as the leader in terms of sales for EVs worldwide [46], and is far more popular in than other EVs combined in Australia [47]. The battery capacity, fuel economy and charging efficiency was therefore assumed to be 85 kWh [48], 0.24 kWh/km [48] and 90% [49] respectively in this study. We modelled the EV penetration rate (*EVPR*) between 0 and 100% (around 16.2 million), in 10% intervals to reflect the potential mid- and long-term EV adoption potential in Australia. The reference case was without EVs, i.e., EVPR=0%. For each *EVPR* >0, we considered EVs both under the uncontrolled and controlled charging. Simulations were undertaken using Matlab 2018b on a high-performance server with 112-Cores CPU and 6TB RAM. Simulating EVs under 100% penetration rate for the whole of Australia with 90×110 raster grid cells over 8760 hours took 17 h for the uncontrolled charging and 23 h for the controlled charging.

3 Results

3.1 Convergence of the integrated grid model

With expensive generators being excluded, the LCOE and overall capacity declines with the iteration of the integrated grid model (see Fig. 3). Our model does not predefine the merit orders during the electricity dispatch, and as a consequence many generators participate during the first iteration, leading to very high LCOE and capacity (Fig. 4). Most of these generators perform poorly, where around 50% of them operate less than 24 hours during one year (8760 h). The curtailment of the uneconomic generators is effective with nearly 90% being excluded

within the first five iterations. The model converges within around 15 iterations, achieving a spatio-temporal grid configuration with minimal LCOE and capacity given the input parameters.

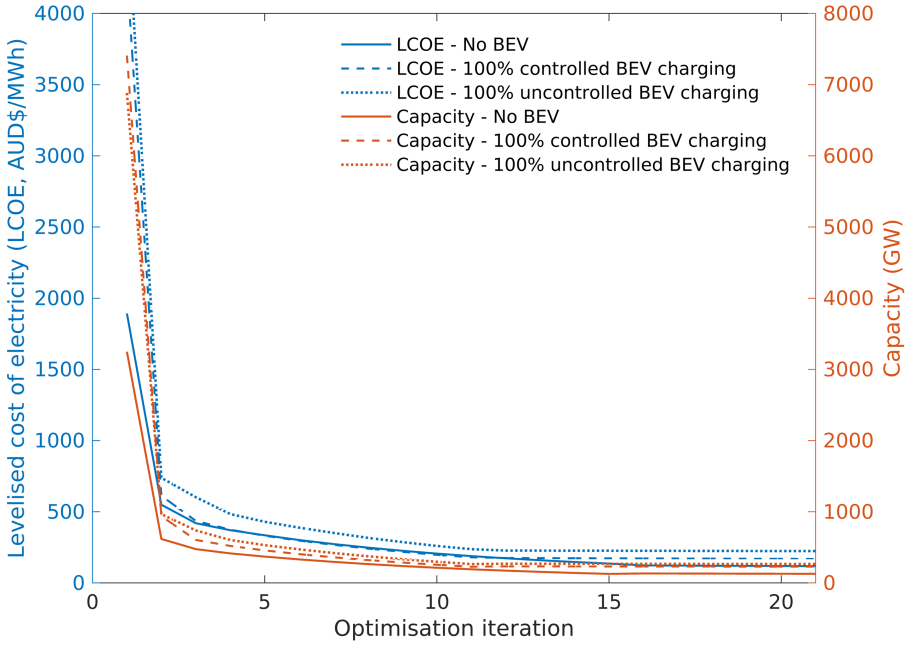

Fig. 3. Levelized cost of electricity (LCOE) and capacity convergence under different EV charging assumptions.

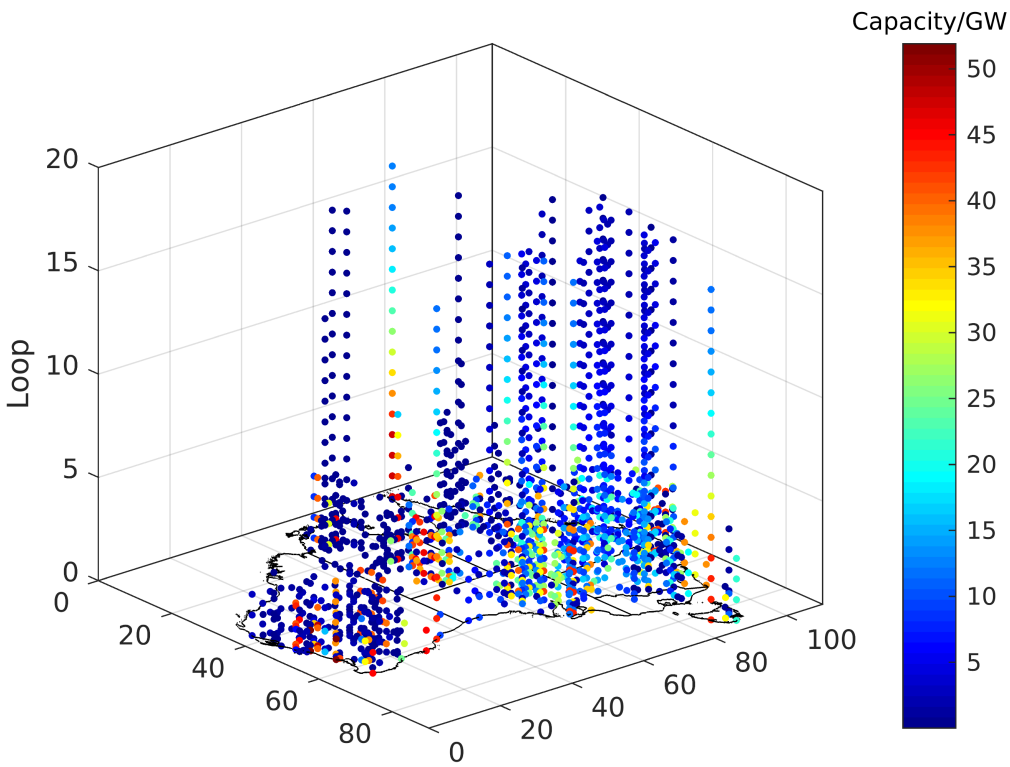

Fig. 4. The convergence of the spatial distribution of generators. *Iteration 1 features both high installed capacity and widely distributed generator sites. As the iterations*

progress, the generator selection narrows down to fewer sites, and installed capacity reduces.

3.2 Impact on installed capacity

EV charging affects both the quantity and the fuel types of the installed capacity of the power grid system (Fig. 5). In the base scenario without EV charging, our model achieves a grid configuration of 143 Gigawatts (GW) installed capacity with wind, PV and CSP contributing 36%, 22% and 36% of the total capacity, respectively. Since the uncontrolled charging load follows the trip arrival time distribution, it peaks around 9:00 in the morning and 18:00 during weekdays, coinciding with current demand peaks (Fig. 8, panel 1). As a result, capacity increases by around 90 GW (around 60%) for accommodating the new demand peak of around 11 GW brought by the uncontrolled EV charging at 100% EVPR.

Due to its low LCOE, wind resource is dispatched first for plugging the demand gap, resulting in an increase of 39 GW in its installed capacity. The solar resource has less availability at 9:00 and 18:00, with only around 20% of the solar intensity during midday. Thus, meeting the additional EV charging demand of 11GW at those two periods requires a high installed capacity of PV and CSP. It leads to a capacity growth of PV by 29 GW and CSP by 20 GW (Fig. 5, top panel).

In contrast, by shifting the charging to periods characterized by high wind and solar resource availability, the controlled charging reduces the total capacity by up to 11% (i.e., 24 GW), compared to the uncontrolled charging with up to 100% EVPR (Fig. 5, bottom panel). Most of the EV charging events offer great flexibility in rescheduling, creating a new charging peak during 12:00-16:00 and increasing the average daily demand peak by up to 5 GW compared to the equivalent uncontrolled charging scenario (Fig. 8, panel 4). As a result, a reduction of up to 11GW in solar-based installed capacity and 12 GW in wind can be achieved by the controlled charging despite the 5GW increase in the demand peak (Fig. 5, bottom panel).

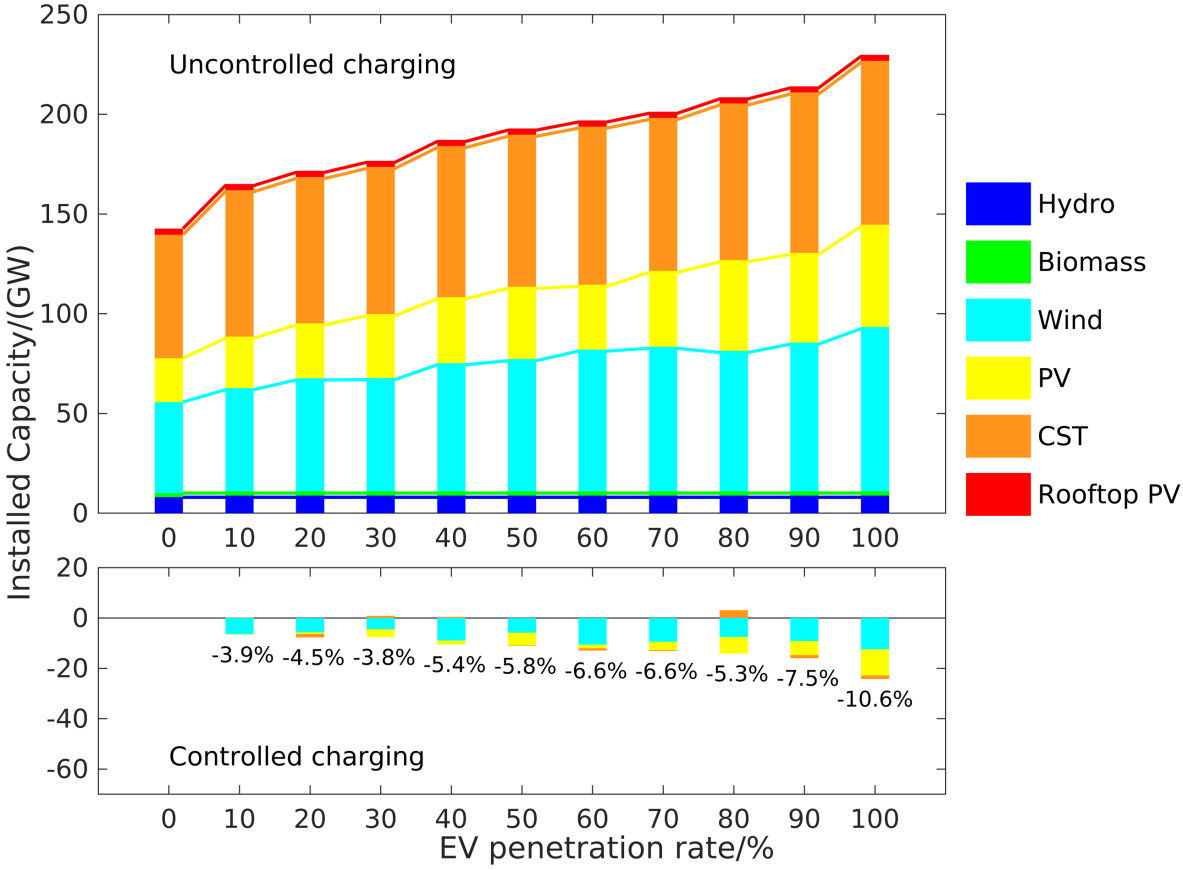

Fig. 5. Installed capacity under uncontrolled and controlled charging. Controlled charging reduces the need for capacity as EV charging demand is moved out of peak periods.

3.3 Impact on LCOE and transmission network

EV charging has a similar effect on LCOE as on installed capacity. Under uncontrolled charging, the LCOE increases by up to 14.6% with EVPR increasing up to 100% (Fig. 6, top panel), where the main growth comes from the capital and fixed O&M (operation and management) cost. This can be understood by examining the optimisation function (Equation 1) where the fixed capital cost measures the capacity-related cost per unit of generation. With uncontrolled EVs charging at the low wind and solar resource availability periods, the system capacity factor drops from nearly 25% (EVPR=0%) to 19% (EVPR=100%), resulting in a higher capacity recruited for generating each unit of output with an increment of the associated fixed-capital cost.

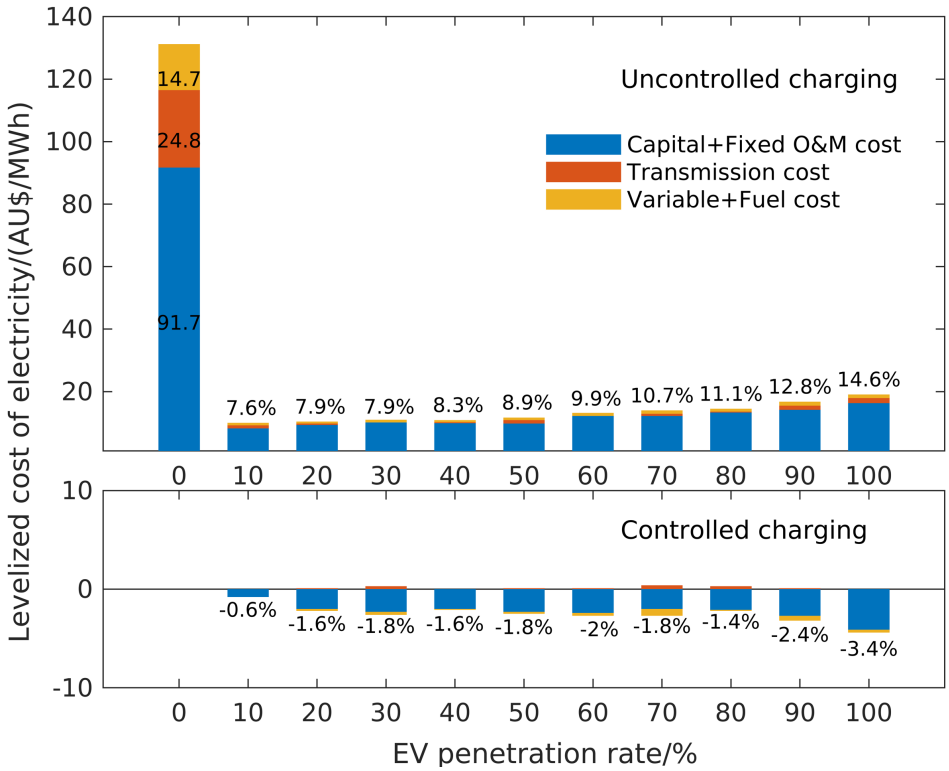

Fig. 6: Effects of uncontrolled and controlled charging on LCOE. Controlled charging reduces predominantly capital and fixed operation and management costs, as it requires less installed capacity (compare with Fig. 5). *10-100: Changes with respect to 0% penetration.*

The increase in transmission and variable fuel costs caused by the unrestricted charging of EVs is small (Fig. 7). This is because uncontrolled charging has little influence on the spatial distribution of the generators. It brings out a similar transmission topology under different EVPRs (see Fig. 7b for the comparison between 100% uncontrolled charging and base scenario).

Under the base scenario without EV charging, the model effectively eliminates most of the wind and PV generators, leaving only those generators in areas with high resources, resulting in wind generators being distributed around the coastline (circles in Fig. 7a) and PV plants being situated in the central desert regions with high solar radiation (squares in Fig. 7a). Due to their 15h heat storage capacity, CSP systems can provide electricity during low solar resource periods and are thus less sensitive to solar resource availability than PV. The positioning of CSP in areas closer to demanders can decrease transmission line losses and thus secure higher bidding competitiveness. As a result of the interplay of both factors – solar resources and

demand location – the recruited CSP plants are located in the more densely populated central east region of the continent (triangles in Fig. 7a).

With uncontrolled charging requiring more installed capacity, an additional capacity of up to around 90 GW increases the total transmission line capacity of up to around 1.8 TW (i.e., 17%), leading to a growth of 6% in transmission cost under 100% EVPR seen in the bottom panel of Fig .6.

Controlled charging can reduce LCOE by up to around 3%-4% compared to the equivalent uncontrolled charging scenario (Fig .6, bottom panel). Fixed capital and O&M costs dominantly contribute to this decrease in LCOE, due to the reduced installed capacity of up to around 10% achieved by controlled charging (Fig. 5, bottom panel). However, since fixed costs measure the capacity-related cost per unit of electricity generation (Equation 1), a considerable difference in installed capacity (of around 10%) can only result in a small change in costs (of around 3%-4%) when divided by the total annual power generation. The total installed capacity is reduced by controlled charging by 24GW with a reduction of total transmission line capacity by around 551 GW (i.e., 4%) compared to the uncontrolled scenario (Fig. 7c).

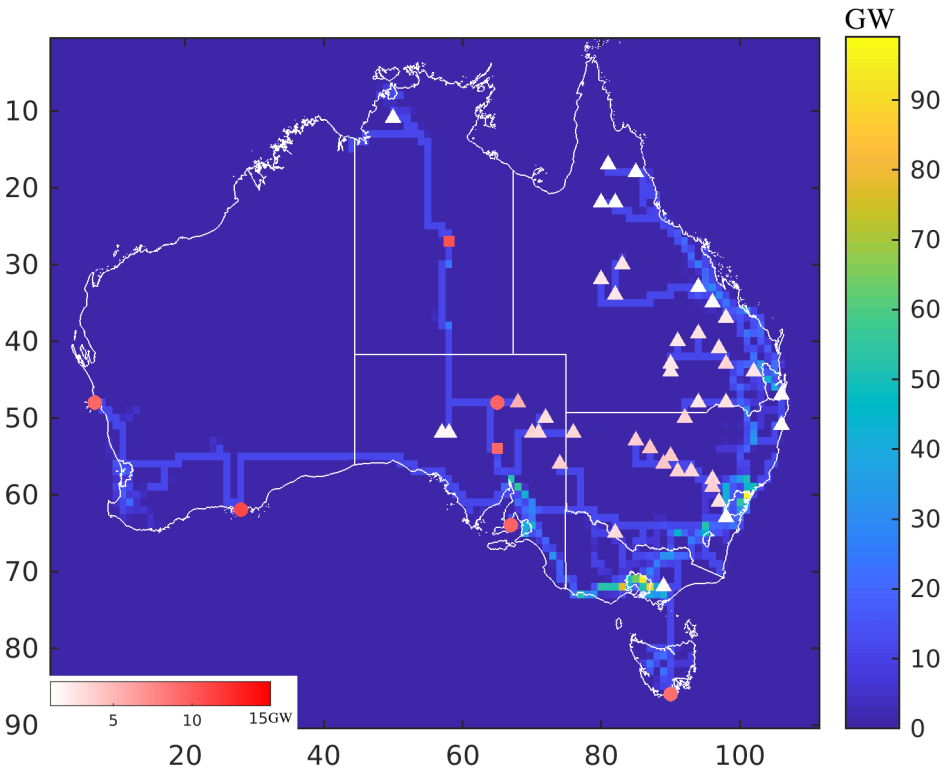

(a) Base scenario without EV charging

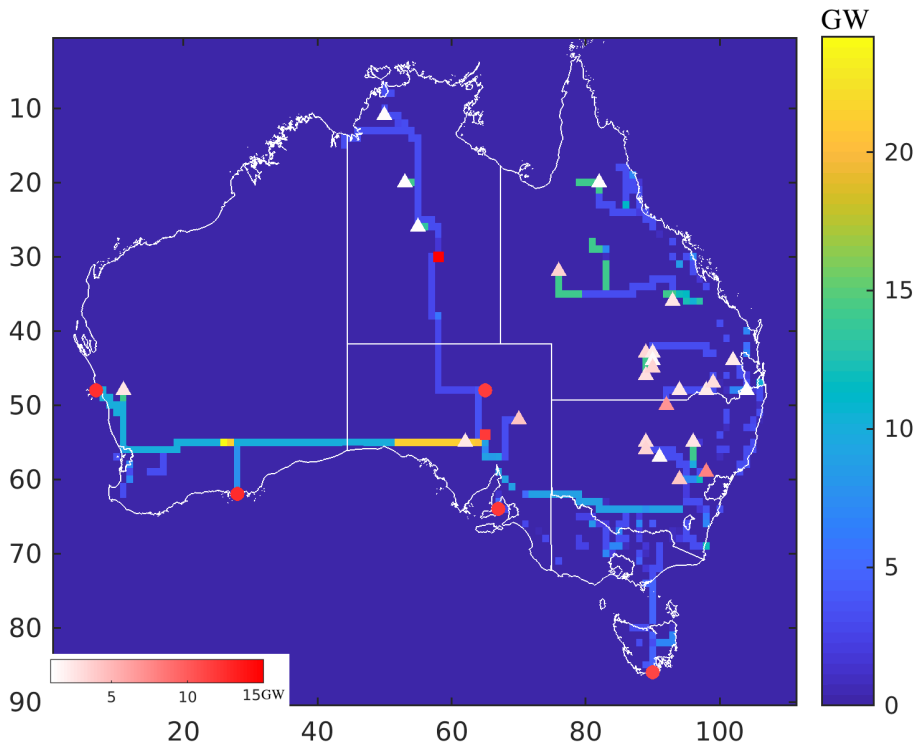

(b) Additional installed capacity and transmission line capacity under 100% uncontrolled EV compared to the base scenario (a).

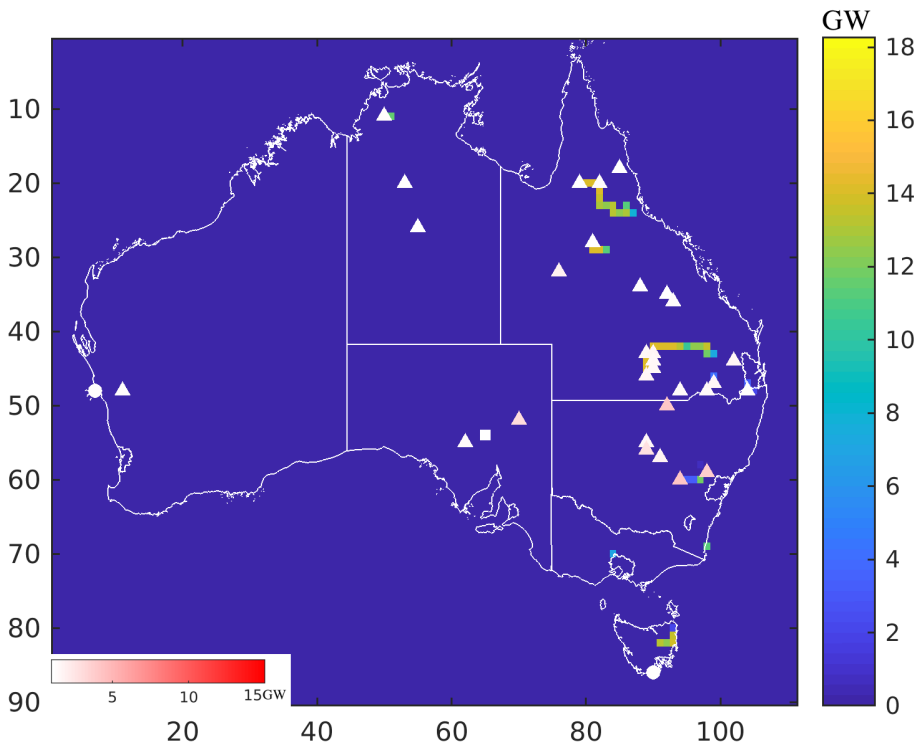

(c) Reduction in installed capacity and transmission line capacity under 100% controlled EV compared to the uncontrolled charging (b).

Fig. 7. Spatial distribution of capacity for generators and transmission network; *The*

blue-to-yellow colour bar indicates the transmission line capacity; The white-to-red colour bar indicates the capacity of generators, where circle=wind, square=PV, and triangle=CSP.

3.4 Hourly profile of electricity generation, spillage, and recruited capacity

We examine the hourly profile of electricity generation, spillage and recruited capacity at a typical summer (Fig. 8a) and winter week (Fig. 8b) to illustrate the hourly dispatch details and how the adoption of RE resources is supported by the controlled charging through shifting the EV charging to high resource availability periods. On weekdays during hours 312~352 and 400~472 in Fig. 8a and 3591~3759 in Fig. 8b), the two-peak periods for EV charging load are in the morning between 8:30 and 9:00 and evening around 18:00 with little or no spillage available (Fig. 8, panel 3). Due to the low wind and solar resource availability, these two peaks necessitate a high system capacity, with nearly 190 GW required for meeting a total demand of 50 GW in winter (Fig. 8b, panel 2), comparing to high solar resource periods between 12:00-16:00 with around only 80GW recruited for a demand of around 40 GW in summer (Fig. 8a, panel 2).

Under controlled EV charging the demand peak can be shifted toward high RE resource periods by substituting the generation of uneconomic generators at low RE resource periods with the spillage of cheap generators. At the same time, the spillage of wind and PV reduces from 22% to 9% (Fig. 8a and b, panels 3, 5 and 7). The hourly recruited capacity peak reduces from 190 GW to around 140GW in a typical winter week (Fig. 8b, panel 9) and 160 GW to around 120 GW in a summer week (Fig. 8a, panel 9).

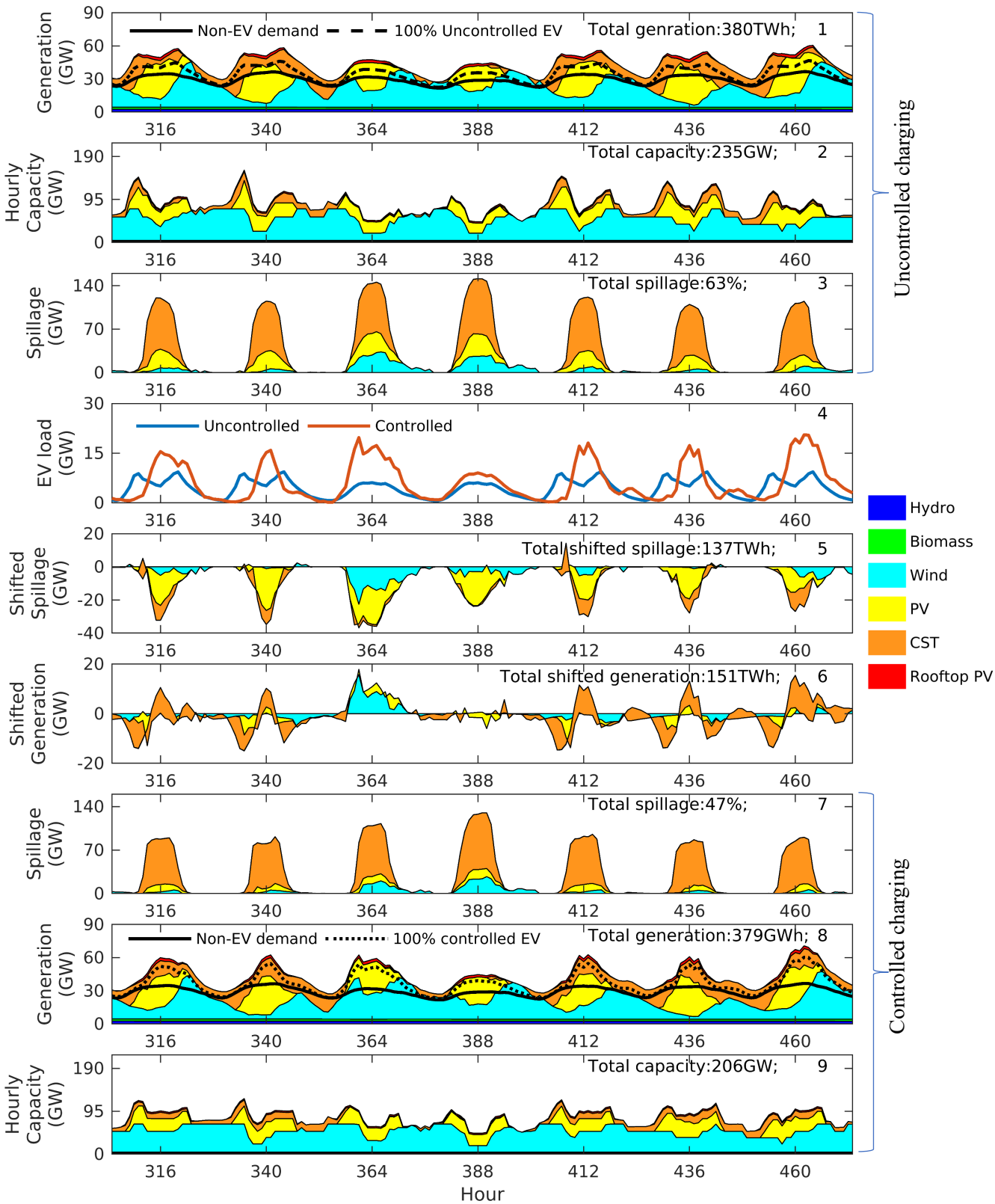

(a) A typical summer week

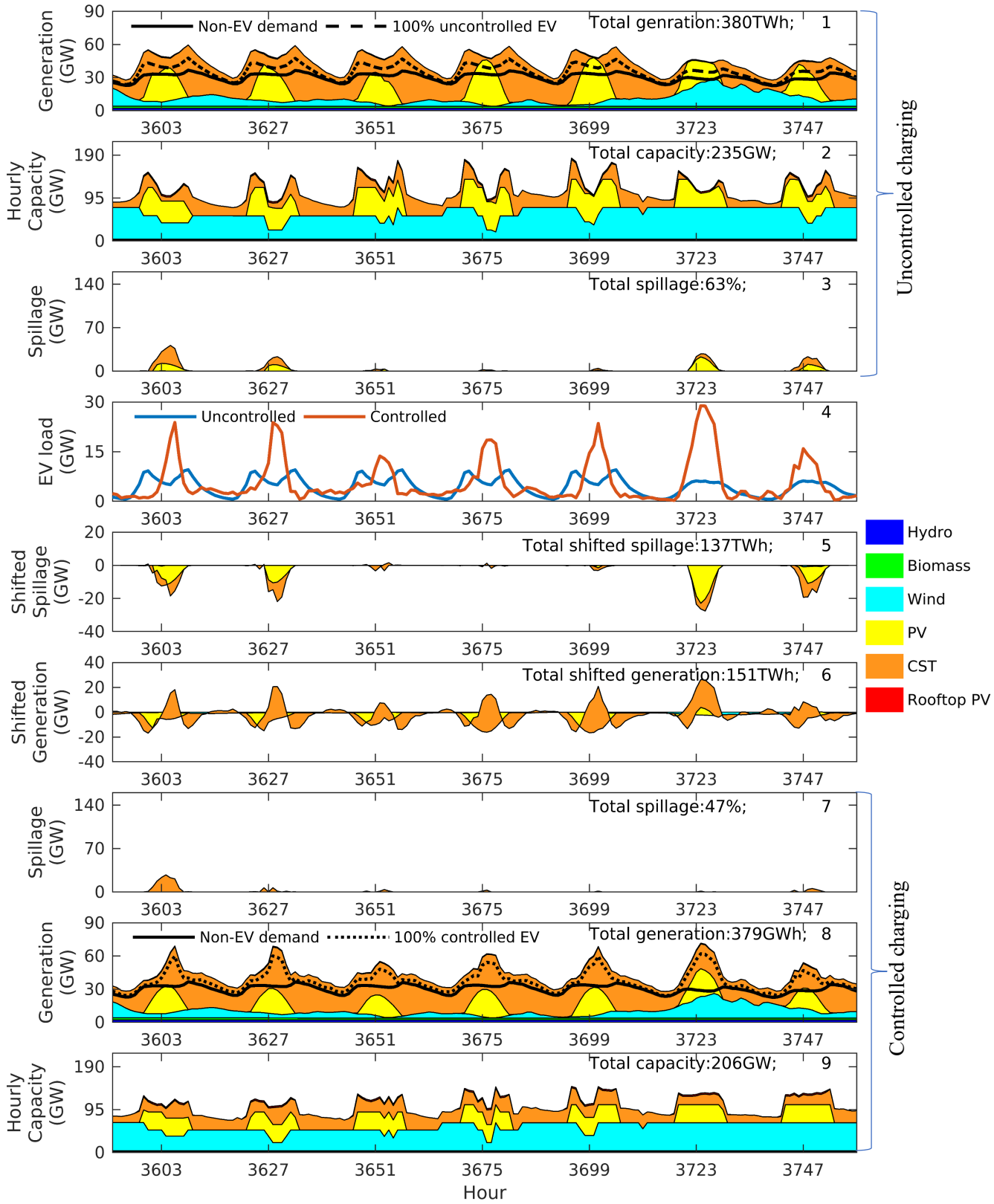

(b) A typical winter week

Fig. 8 Hourly profile for electricity dispatch under 100% EV penetration. *Panels 1-3 and 7-9 show the hourly generation, recruited installed capacity and spillage before and after*

controlled charging; Panel 4 compares the EV charging load under uncontrolled and controlled charging; Panels 5-6 present the hourly shifted spillage and generation by controlled charging.

4 Discussions and conclusions

This study identifies the three LCOE under different system installed capacity: 13.5 AUD¢/kWh with 143 GW capacity for no EV charging (reference scenario), 15.0 AUD¢/kWh with 229 GW capacity for uncontrolled EV charging, and 14.7 AUD¢/kWh with 205 GW capacity for controlled EV charging. All scenarios realise a 100 % renewable electricity system in Australia, including following demonstrated low carbon technologies: hydro, wind, concentrating solar, rooftop, utility PV, and biomass.

The results of the reference scenario can be compared with earlier simulations on 100% RE supply in Australia [34, 50, 51], identifying about 83-110 GW installed capacity at an LCOE of 9.6-11.1 AUD¢/kWh. A combination of factors cause those differences in installed capacity and LOCE: 1) we include the Northern Territory and Western Australia, leading to about a 15% increase); 2) we restrict the capacity expansion of dispatchable resources such as biomass and hydro, which account for 26%-37% in total capacity in [34, 50, 51] and 6% in our study.

With an average fuel consumption rate of 13.1 L/100km [52] and fuel cost of 141.1 AUD¢/L [53] across all Australian vehicles, the average cost for conventional vehicles is estimated to be 18.5 AUD¢/km. This leads to an annual average fuel cost of 2,484 AUD considering a yearly travel distance of 13,440 km per vehicle [39]. Using 0.8 vehicle per capita in Australia [54], the annual fuel cost is 1,987 AUD/capita. With an annual residential electricity consumption of 2,133 kWh/capita (Table 2, [55, 56]) at a price of around 30 AU¢/kWh [57], annual expenditures for electricity (640 AU$) and fuel (1,987 AU$) are 2,627 AU$ per capita (Table 3, 2nd column). Assuming a linear relationship between electricity retailer price and LCOE, transitioning to a 100% RE grid would increase the electricity retailer price to round 33 AU¢/kWh [58]. Referring to Tesla's energy mileage (24 kWh/100km [48]) the fuel cost for electric vehicles becomes 844 AU$/capita, and the residential electricity cost for 2,133 kWh/capita becomes 698 AU$/capita (Table 3, 3rd column). In total, the annual expenditure on vehicles and electricity reduces to 1,541 AU$/capita, which is entirely due to a reduction is transport cost. Therefore, we find that transitioning to a 100% RE supply with EV charging has

potential annual cost savings around 1,000 AU$/capita.

Table 1. National overview of the Australian electricity consumption [55, 56].

National overview on the Australian electricity consumption			
Residential		Industrial	
192	PJ	713	PJ
53.3	TWh	198.3	TWh
2,133	kWh/cap	7,933	kWh/cap
30	AU¢/kWh	27	AU¢/kWh
640	AU$/cap/y	2,244	AU$/cap/y
16.0	**AU$b/year**	**56.1**	**AU$b/year**

Table 2. Cost comparison between current fuel and electricity costs with 100% EVs under 100% RE supply.

Transport energy	**Liquid fuels**		**100% RE Electricity**		**Difference**
Energy efficiency	13.1 [52]	L/100km	24.0 [48]	kWh/100km	
Annual mileage	13440.0 [38]	km/veh	13440.0	km/veh	
Energy consumption	1760.6	L/veh	3225.6	kWh/veh	
Energy price	141.1 [53]	AU¢/L	32.7 [58]	AU¢/kWh	
Vehicle energy cost	2484.3	AU$/veh	1054.8	AU$/veh	
Vehicle ownership	0.8 [54]	veh/cap	0.8	veh/cap	
Per-capita energy cost	**1,987**	**AU$/cap/y**	**844**	**AU$/cap/y**	**-1,144**

Residential electricity	**Current grid**		**Current grid**		**Difference**
Total energy consumption	192.0	PJ	192.0	PJ	
Per-capita energy consumption	2133.0	kWh/cap	2133.0	kWh/cap	
Energy price	30.0	AU¢/kWh	32.7	AU¢/kWh	
Per-capita energy cost	**640**	**AU$/cap/y**	**698**	**AU$/cap/y**	**57.6**

Summary	**Current grid**		**Current grid**		**Difference**
Transport energy	1987.4	AU$/cap/y	843.8	AU$/cap/y	
Residential electricity	639.9	AU$/cap/y	697.5	AU$/cap/y	
Total per-capita energy cost	**2,627**	**AU$/cap**	**1,541**	**AU$/cap**	**-1,086**

For future studies, different technology adoption percentages for example with more widespread availability of dispatchable resources (e.g., hydro, biomass or electrical energy storage [59] deployed in future power system would change the RE-based grid's LCOE and installed capacity features, thus allowing for multiple transition and policy scenarios to be appraised. Our model enables evaluating the LCOE under configurations with various dispatchable energy resources, which remains as a future task. Our model can also be used to further analyze the impact of introducing vehicle-to-grid technology in Australia on power generation, transmission and distribution, and the associated system LOCE.

ACKNOWLEDGMENT

The authors would like to thank Tommy Wiedmann and Daniel Micevski from the School of Civil and Environmental Engineering at University of New South Wales and Arne Geschke for managing the access to the high-performance computer, and the Chinese Scholarship Council for providing a PhD scholarship.

REFERENCES

[1] Rogelj J, D. Shindell, K. Jiang, S. Fifita, P. Forster, V. Ginzburg, C. Handa, H. Kheshgi, S. Kobayashi, E. Kriegler, L. Mundaca, R. Séférian, and M.V. Vilariño,. . Rogelj, J., D. Shindell, K. Jiang, S. Fifita, P. Forster, V. Ginzburg, C. Handa, H. Kheshgi, S. Kobayashi, E. Kriegler, L. Mundaca, R. Séférian, and M.V. Vilariño,Mitigation Pathways Compatible with 1.5°C in the Context of Sustainable Development. In: Global Warming of 1.5°C. An IPCC Special Report on the impacts of global warming of 1.5°C above pre-industrial levels and related global greenhouse gas emission pathways, in the context of strengthening the global response to the threat of climate change, sustainable development, and efforts to eradicate poverty. 2018.

[2] IEA. CO2 Emissions From Fuel Combustion Highlights 2014. OECD Publishing: International Energy Agency (IEA); 2014.

[3] International Energy Agency (IEA). Energy Technology Perspectives 2017: Catalyzing Energy Technology Transformations. Paris, France2017.

[4] Hill G, Heidrich O, Creutzig F, Blythe P. The role of electric vehicles in near-term mitigation pathways and achieving the UK' s carbon budget. Applied Energy. 2019;251:113111.

[5] Budischak C, Sewell D, Thomson H, MacH L, Veron DE, Kempton W. Cost-minimized

combinations of wind power, solar power and electrochemical storage, powering the grid up to 99.9% of the time. Journal of Power Sources. 2013;225:60-74.

[6] Richardson DB. Electric vehicles and the electric grid: A review of modeling approaches, Impacts, and renewable energy integration. Renewable and Sustainable Energy Reviews. 2013;19:247-54.

[7] Zhang W, Gandhi O, Quan H, Rodríguez-Gallegos CD, Srinivasan D. A multi-agent based integrated volt-var optimization engine for fast vehicle-to-grid reactive power dispatch and electric vehicle coordination. Applied Energy. 2018;229:96-110.

[8] Wu D, Radhakrishnan N, Huang S. A hierarchical charging control of plug-in electric vehicles with simple flexibility model. Applied Energy. 2019;253:113490.

[9] Seddig K, Jochem P, Fichtner W. Two-stage stochastic optimization for cost-minimal charging of electric vehicles at public charging stations with photovoltaics. Applied Energy. 2019;242:769-81.

[10] Lin H, Liu Y, Sun Q, Xiong R, Li H, Wennersten R. The impact of electric vehicle penetration and charging patterns on the management of energy hub – A multi-agent system simulation. Applied Energy. 2018;230:189-206.

[11] Jian L, Zheng Y, Xiao X, Chan CC. Optimal scheduling for vehicle-to-grid operation with stochastic connection of plug-in electric vehicles to smart grid. Applied Energy. 2015;146:150-61.

[12] Wang D, Guan X, Wu J, Li P, Zan P, Xu H. Integrated Energy Exchange Scheduling for Multimicrogrid System With Electric Vehicles. IEEE Transactions on Smart Grid. 2016;7:1762-74.

[13] Morais H, Sousa T, Vale Z, Faria P. Evaluation of the electric vehicle impact in the power demand curve in a smart grid environment. Energy Conversion and Management. 2014;82:268-82.

[14] Madzharov D, Delarue E, D'Haeseleer W. Integrating electric vehicles as flexible load in unit commitment modeling. Energy. 2014;65:285-94.

[15] Wang D, Gao J, Li P, Wang B, Zhang C, Saxena S. Modeling of plug-in electric vehicle travel patterns and charging load based on trip chain generation. Journal of Power Sources. 2017;359:468-79.

[16] Nikoobakht A, Aghaei J, Khatami R, Mahboubi-Moghaddam E, Parvania M. Stochastic flexible transmission operation for coordinated integration of plug-in electric vehicles and renewable energy sources. Applied Energy. 2019;238:225-38.

[17] Abbasi MH, Taki M, Rajabi A, Li L, Zhang J. Coordinated operation of electric vehicle charging and wind power generation as a virtual power plant: A multi-stage risk constrained approach. Applied Energy. 2019;239:1294-307.

[18] Valentine K, Temple WG, Zhang KM. Intelligent electric vehicle charging: Rethinking the valley-fill. Journal of Power Sources. 2011;196:10717-26.

[19] Weis A, Jaramillo P, Michalek J. Estimating the potential of controlled plug-in hybrid electric vehicle charging to reduce operational and capacity expansion costs for electric power systems with high wind penetration. Applied Energy. 2014;115:190-204.

[20] Paevere P, Higgins A, Ren Z, Horn M, Mcnamara C. Spatio-temporal modelling of electric vehicle charging demand and impacts on peak household electrical load. Sustainability Science. 2014;9.

[21] Mu Y, Wu J, Jenkins N, Jia H, Wang C. A Spatial–Temporal model for grid impact analysis of plug-in electric vehicles. Applied Energy.114:456-65.

[22] Gennaro MD, Paffumi E, Scholz H, Martini G. GIS-driven analysis of e-mobility in urban areas: An evaluation of the impact on the electric energy grid. Applied Energy. 2014;124:94–116.

[23] Willis, H.L. Spatial Electric Load Forecasting [Book Review]. Computer Applications in Power IEEE.10:58-9.

[24] Hedegaard K, Ravn H, Juul N, Meibom P. Effects of electric vehicles on power systems in Northern Europe. Energy. 2012;48:356-68.

[25] Hanemann P, Behnert M, Bruckner T. Effects of electric vehicle charging strategies on the German power system. Applied Energy. 2017;203:608-22.

[26] Taljegard M, Göransson L, Odenberger M, Johnsson F. Impacts of electric vehicles on the electricity generation portfolio – A Scandinavian-German case study. Applied Energy. 2019;235:1637-50.

[27] Haque ANMM, Ibn Saif AUN, Nguyen PH, Torbaghan SS. Exploration of dispatch model integrating wind generators and electric vehicles. Applied Energy. 2016;183:1441-51.

[28] O'Sullivan D, Perry GLW. Spatial Simulation: Exploring Pattern and Process2013.

[29] The Renewable Energy Target (RET) scheme. 23 June 2015; https://www.environment.gov.au/climate-change/government/renewable-energy-target-scheme.

[30] Government of South Australia. A low carbon investiment plan for South Australia 2015.

[31] ACT Government. 100% renewable energy for Canberra by 2020. 2016.

[32] ENERGEIA. Australian Electric Vehicle Market Study. ENERGEIA; 2018.

[33] Short W, Sullivan; P, Mai; T, Mowers; M, Martinez CUNBDHaA. Regional Energy Deployment System (ReEDS). Technical Report NREL/TP66A20646534, Golden, USA, National Renewable Energy Laboratory. 2011.

[34] AEMO. 100 per cent renewables study D modelling outcomes. Australian Energy Market Operator. 2013.

[35] Orr KaNS. National Power Stations Database,Geoscience Australia. 2014.

[36] APVI. Solar Map: Mapping Australian Photovoltaic installations. Australian PV Institute. 2014.

[37] Jing H. Dynamic downscaling of Australian climate for solar energy resource assessment using CCAM. In: AMOS national conference 2014, 12–14 February 2014. Hobart, Australia; 2014. AMOS national conference. Hobart, Australia2014.

[38] https://data.qld.gov.au/dataset/2009-12-south-east-queensland-household-travel-survey. Household Travel Survey. 2012; https://data.qld.gov.au/dataset/2009-12-south-east-queensland-household-travel-survey.

[39] AEMO. Aggregated Price and Demand Data - Historical. 2014a.

[40] Lenzen M, McBain B, Trainer T, Jütte S, Rey-Lescure O, Huang J. Simulating low-carbon electricity supply for Australia. Applied Energy. 2016;179:553-64.

[41] Yousefzadeh M, Lenzen M. Performance of concentrating solar power plants in a whole-of-grid context. Renewable and Sustainable Energy Reviews. 2019;114:109342.

[42] Li M, Lenzen M, Yousefzadeh M, Ximenes F. The roles of biomass and CSP in a 100 % renewable electricity supply in Australia. IEEE Transactions on Sustainable Energy. 2019. (Under review).

[43] Li M, Lenzen M, Keck F, McBain B, Rey-Lescure O, Li B, et al. GIS-Based Probabilistic Modeling of BEV Charging Load for Australia. IEEE Transactions on Smart Grid. 2019;10:3525-34.

[44] Li M, Lenzen M. How many electric vehicles can the current Australian electricity grid support? International Journal of Electrical Power & Energy Systems. 2020;117:105586.

[45] Shen L, Fields S, Stopher P, Zhang Y. The Future Direction of Household Travel Surveys in Australia. Australasian Transport Research Forum (ATRF), 38th, 2016, Melbourne, Victoria, Australia; 2016.

[46] Battery-electric vehicle sales worldwide. 2018; https://www.statista.com/statistics/666130/global-sales-of-electric-vehicles-ytd-by-brand/.

[47] Australian Electric Vehicle Market Study. May 2018. p41; https://arena.gov.au/assets/2018/06/australian-ev-market-study-report.pdf.

[48] United States Environmental Protection Agency and U.S. Department of Energy. Fuel Economy Guide – Electric vehicles & Plug-in Hybrid Electric Vehicles 2018. p. 32.

[49] Li M, Zhang X, Li G. A comparative assessment of battery and fuel cell electric vehicles using a well-to-wheel analysis. Energy. 2016;94:693-704.

[50] Elliston B, MacGill I, Diesendorf M. Least cost 100% renewable electricity scenarios in the

Australian National Electricity Market. Energy Policy. 2013;59:270-82.

[51] Blakers A, Lu B, Stocks M. 100% renewable electricity in Australia. Energy. 2017;133:471-82.

[52] Australian Government, Department of Infrastructure and Regional Development. Fuel economy of Australian passenger vehicles – a regional perspective. 2017.

[53] Australian Competition and Consumer Commission. Report on the Australian petroleum market. 2019.

[54] Australian Bureau of Statistics. 9309.0 - Motor Vehicle Census, Australia. 31 Jan 2019.

[55] Australian Bureau of Statistics. 5209.0.55.001 - Australian National Accounts: Input-Output Tables, 2014-15. .

[56] Australia Government Department of Industry, Science, Energy and Resources. Resources and Energy Quarterly – March 2020.

[57] Australian Competition and Consumer Commission. Restoring electricity affordability and Australia' s competitive advantage. 2018.

[58] Australian Energy Market Commission. 2018 Residential Electricity Price Trends Review. 21 DECEMBER 2018.

[59] Keck F, Lenzen M, Vassallo A, Li M. The impact of battery energy storage for renewable energy power grids in Australia. Energy. 2019;173:647-57.

Appendix:

Table A1. System installed capacity for uncontrolled and controlled charging scenarios by penetration rates

EV penetration rate	Installed capacity for uncontrolled charging (GW)				LCOE for controlled charging (GW)			
	Wind	PV	CSP	Total capacity	Wind	PV	CSP	Total capacity
0%	46	22	62	143	46	22	62	143
10%	52	26	73	164	45	26	74	158
20%	57	28	73	171	51	27	72	163
30%	57	32	74	176	52	29	75	169
40%	64	33	76	186	55	32	76	176
50%	66	36	76	192	61	31	76	181
60%	71	32	79	196	61	31	78	183
70%	73	38	77	200	63	35	76	187
80%	70	46	79	208	63	39	82	197
90%	75	45	80	213	66	39	79	197
100%	82	51	82	229	70	41	81	205

Table A2: System LCOE for uncontrolled and controlled charging scenarios by penetration rates

EV penetration rate	LCOE for uncontrolled charging (A$/MWh)				LCOE for controlled charging (A$/MWh)			
	Capacity & Fixed cost	Transmission cost	Variable & Fuel cost	Total LCOE	Capacity & Fixed cost	Transmission cost	Variable & Fuel cost	Total LCOE
0%	91.7	24.8	14.7	131.2	91.7	24.8	14.7	131.2
10%	99.9	25.8	15.5	141.2	99.1	25.8	15.5	140.4
20%	101.0	25.3	15.3	141.6	99.0	25.4	15.1	139.5
30%	101.8	24.2	15.6	141.6	99.5	24.5	15.3	139.3
40%	101.6	25.1	15.4	142.1	98.4	25.1	15.3	138.8
50%	101.5	25.9	15.5	142.9	99.2	26.0	15.3	140.5
60%	103.9	24.6	15.7	144.2	101.5	24.7	15.4	141.6
70%	104.0	25.1	15.7	144.8	101.6	25.9	15.1	142.6
80%	105.0	25.1	15.6	145.7	101.6	25.4	15.5	142.5

90%	105.9	26.1	16.0	147.9	103.2	26.2	15.5	144.9
100%	108.0	26.4	15.9	150.3	103.9	26.4	15.6	145.9